Research Article

Optimization of Preparation of Activated Carbon from *Ricinus communis* Leaves by Microwave-Assisted Zinc Chloride Chemical Activation: Competitive Adsorption of Ni^{2+} Ions from Aqueous Solution

M. Makeswari and T. Santhi

Department of Chemistry, Karpagam University, Tamil Nadu, Coimbatore 641021, India

Correspondence should be addressed to T. Santhi; ssnilasri@yahoo.co.in

The preparation of activated carbon (AC) from *Ricinus communis* leaves was investigated in this paper. Orthogonal array experimental design method was used to optimize the preparation of AC using microwave assisted zinc chloride. Optimized parameters were radiation power of 100 W, radiation time of 8 min, concentration of zinc chloride of 30% by volume, and impregnation time of 24 h, respectively. The surface characteristics of the AC prepared under optimized conditions were examined by pH$_{ZPC}$, SEM-EDAX, XRD, and FTIR. Competitive adsorption of Ni^{2+} ions on *Ricinus communis* leaves by microwave assisted zinc chloride chemical activation (ZLRC) present in binary and ternary mixture was compared with the single metal solution. The effects of the presence of one metal ion on the adsorption of the other metal ion were investigated. The experimental results indicated that the uptake capacity of one metal ion was reduced by the presence of the other metal ion. The extent of adsorption capacity of the binary and ternary metal ions tested on ZLRC was low (48–69%) as compared to single metal ions. Comparisons with the biosorption of Ni^{2+} ions by the biomass of ZLRC in the binary (48.98–68.41%-~Ni-Cu and 69.76–66.29%-~Ni-Cr) and ternary solution (67.32–57.07%-~Ni–Cu and Cr) could lead to the conclusion that biosorption of Ni^{2+} ions was reduced by the influence of Cu^{2+} and Cr^{3+} ions. The equilibrium data of the adsorption was well fitted to the Langmuir isotherm. The adsorption process follows the pseudo-second-order kinetic model.

1. Introduction

The pollution of water resources due to the indiscriminate disposal of heavy metals has been causing worldwide concern for the last few decades. It is well known that some metals can have toxic or harmful effects on many forms of life. Among the most toxic metals are chromium (Cr), copper (Cu), lead (Pb), zinc (Zn), and mercury (Hg), which is one of the 11 hazardous priority substances in the list of pollutants contained in the Water Framework Directive (Directive 2000/60/EC) [1]. Many industries discharge heavy metals such as lead, cadmium, copper, nickel, and zinc in their waste waters [2]. Among these metals Ni is known to be essential to plants, humans, and animals, but they can also have adverse effects if their availability in water exceeds certain threshold values. Therefore, the removal of such heavy metals from waste streams before discharge to public water sources is of primary concern.

Some workers indicated that precipitation is a suitable method for metal removal from wastewaters containing high concentrations of heavy metals [3]. In some cases, ion exchange and activated carbon adsorption have been used [4, 5]. Electrochemical treatment, membrane process, and biological methods are also used. However, these methods become noneconomical when dealing with very small concentrations of metals due to the need to use expensive monitoring systems. Adsorption is considered to be one of the most economical and effective methods for removal of

metals from wastewaters. Activated carbon was widely used in the removal of dyes and metals from industrial waste waters, which had relatively high sorption capacity for a wide variety of dyes and metals.

Activated carbons (AC) are an amorphous form of carbon, characterized by high internal porosity and consequently high adsorptivity. It has wide applications like removal of organic, inorganic pollutants from drinking water and as catalyst support [6]. Adsorption capacity of activated carbon strongly depends on its porosity and surface area. Textural property of AC depends on method of preparation and starting material [7]. Generally, two methods are used for the preparation of AC via physical and chemical activation. During physical activation, the raw material is carbonized first at high temperature and then it is activated by CO_2 or steam under pressure to increase porosity and surface area of AC. In chemical activation both carbonization and activation takes place simultaneously, in which raw material is first impregnated with activating chemical and then carbonized at desired temperature that varies according to activating chemical used [6]. Chemical activation is held in presence of dehydrating reagents such as KOH, K_2CO_3, NaOH, $ZnCl_2$, and H_3PO_4 which influence pyrolytic decomposition and inhibit tar formation. The carbon yield obtained is higher and the temperature used in chemical activation is lower than that of physical activation. Behaviors of the reagents during chemical activation show different effects on the final product. $ZnCl_2$ is widely used as activating reagent, since it resulted in high surface areas and high yield [8, 9]. In the use of $ZnCl_2$, the activated carbons had large surface areas and more micropore structure [10, 11].

AC with high surface area and porosity can be prepared from many lignocellulosic materials such as coal, coconut shell [7, 12] wood, agricultural waste saw dust, cashew nut shell, and jackfruit feel waste. Researcher's interest is growing in the use of other low cost and abundantly available lingocellulosic material as a precursor for the preparation of AC [10–14]. Adsorption capacity of prepared activated carbons especially for metal ion depends on a number of acidic/ polar oxygen functional groups present on its surface. For preparing activated carbon, conventional heating method is usually adopted, in which the energy is produced by electrical furnace. Recently, microwave heating technology has been applied to fabricate activated carbon due to its rapid heating and uniformity [15].

The application of microwave (MW) heating technology for regenerating industrial waste activated carbon has been investigated with very promising results [15, 16]. The main difference between MW devices and conventional heating systems is the way of heat generated. In the MW device, the microwaves supply energy directly to the carbon bed. Energy transfer is not by conduction or convection as in conventional heating, but microwave energy is readily transformed heat into inside the particles by dipole rotation and ionic conduction [15–17].

The aim of the present work was to optimize the ZLRC preparation conditions using orthogonal array experimental design method, investigate the ability of a nickel sorbent prepared from *Ricinus communis* leaves, and study the effect

Table 1: Design factors and levels.

Independent variables	Symbol	Range and levels			
		1	2	3	4
Radiation power (W)	A	100	200	400	600
Radiation time (min)	B	4	6	8	10
Concentration of $ZnCl_2$ (vol%)	C	30	40	50	60
Impregnation time (h)	D	16	20	24	28

of several parameters (pH, contact time, initial metal concentration, pH_{ZPC}, and foreign ions effect) on the adsorption efficiency of nickel from aqueous solution.

2. Experimental Section

2.1. Materials. The *Ricinus communis* leaves were obtained from an agricultural form in Tirupur district (Tamil Nadu). It was air-dried and powdered in a grinder and then it was used for further experimental studies. Samples of zinc chloride ($ZnCl_2$), hydrochloric acid (HCl), sodium hydroxide (NaOH), and nickel sulphate hexa hydrate ($NiSO \cdot 6H_2O$) were obtained from Aluva, Edayar (specrum reagents and chemicals pvt. Ltd.). All other chemicals used in this study were analytical grade and purchased from Aluva, Edayar (spectrum reagents and chemicals pvt. Ltd.).

2.2. Preparation of Stock Solution. Nickel stock standard solution (1000 mg/L) was prepared from a readymade nickel sulphate hexa hydrate ($NiSO_4 \cdot 6H_2O$) standard. Working nickel solutions were prepared just before used by appropriate dilutions of stock solution.

2.3. Preparation of ZLRC. The *Ricinus communis leaves* were obtained from the agricultural form in Tirupur district (Tamil Nadu). It was air-dried and powdered in a grinder. Dried *Ricinus communis* with the mass of 6 g were mixed with 30 mL of $ZnCl_2$ to vary concentrations in the range of 30–60% by volume. The slurry was kept at room temperature for various time spans in the range of 16–28 h to ensure the access of the $ZnCl_2$ to the *Ricinus communis leaves*. After mixing, the slurry was placed in a MW heating apparatus (MW71E, SAMSUNG). After a certain microwave heating power and microwave radiation time, the carbonized samples were washed with 0.5 M HCl, hot water, and cold distilled water until the pH of the washing solution reached 6-7, filtered, and finally dried at 150°C.

2.4. Optimization of ZLRC Preparation Conditions. In order to optimize the preparation conditions of the ZLRC, Taguchi experimental design method was used [18]. An L_{16} orthogonal array with four operational parameters each in four levels was used to evaluate the corresponding optimal values. These variables and their values are summarized in Table 1. The complete design matrix of the experiments and the obtained results are shown in Table 2. Iodine is considered as probe molecules for assessing the adsorption capacity of adsorbents for solutes of molecular sizes less than 10 Å. Iodine number

TABLE 2: Experimental design matrix and results.

Runs	Variables				Responses (Y)	
	A	B	C	D	Yield (Y_1, %)	Iodine number (Y_2, mg/g)
1	1	1	1	1	49.43	735.50
2	2	1	1	1	55.51	898.97
3	3	1	1	1	56.40	980.70
4	4	1	1	1	41.69	940.40
5	1	1	1	1	35.64	1389.30
6	1	2	1	1	48.64	1307.60
7	1	3	1	1	48.57	1552.97
8	1	4	1	1	47.85	13207.6
9	1	1	1	1	45.79	898.40
10	1	1	2	1	46.95	1062.10
11	1	1	3	1	49.90	1144.10
12	1	1	4	1	43.13	1062.10
13	1	1	1	1	49.43	735.50
14	1	1	1	2	52.52	980.67
15	1	1	1	3	58.34	1225.87
16	1	1	1	4	56.18	1144.10

was normally listed as specification parameter for ZLRC. Therefore, the responses were yield (Y_1, %), and the iodine number (Y_2, mg/g) was obtained at $25 \pm 1°C$ on the basis of the standard Test method. The yield of the carbon samples was estimated according to

$$Y = \frac{M}{M_0} \times 100, \qquad (1)$$

where M is the weight of ZLRC and M_0 is the weight of air-dried *Ricinus communis* leaves.

2.5. Characterization of ZLRC. The surface physical morphology of ZLRC was identified by using SEM technique (Jeol jsm-6390). A Fourier transform infrared spectroscopy (SHIMADZU, IR Affinity-1) with KBr pellet was used to study the surface functional groups of the ZLRC, with a scanning range of 4000–400 cm^{-1}. The crystalline structure of ZLRC was evaluated by XRD analysis. The point of zero surface charge characteristic of ZLRC was (pH$_{ZPC}$) determined by using the solid addition method [19].

2.6. Batch Equilibrium Studies. To study the effect of parameters such as adsorbent dose, metal ion concentration, and solution pH for the removal of adsorbate on ZLRC, batch experiments were performed. Stock solutions of nickel were prepared by dissolving NiSO$_4$·6H$_2$O in deionized water and further diluted to the 50–200 mg/L concentrations for the experiments. pH was adjusted by adding 0.1 M HCl or 0.1 M NaOH into the solutions with known initial nickel ion concentrations. Batch adsorption experiments were conducted in asset of 250 mL stoppered flasks containing 0.2 g of ZLRC and 50 mL of metal solutions with different concentrations (50, 100, 150, and 200 mg/L) at pH 7. The flasks were agitated using a mechanical orbital shaker, and maintained at room temperature for 2 h until the equilibrium was reached. The

suspensions were filtered and metal concentrations in the supernatant solutions were measured using a UV-vis spectrophotometer at 232 nm. The amount of uptake of Ni^{2+} ions by ZLRC in the equilibrium (q_e) was calculated by the following mass-balance relationship:

$$q_e = \frac{(C_0 - C_e)}{W} \times V, \qquad (2)$$

where C_o and C_e (mg/L) are the liquid phase concentrations of metal at initial and equilibrium, respectively. V (L) is the volume of the solution, and W (g) is the mass of adsorbent used. We used different models, Langmuir, Freundlich, Temkin, and Dubinin-Radushkevich to investigate the equilibrium behavior of Ni^{2+} ion adsorption on the prepared ZLRC samples.

2.7. Batch Kinetic Studies. The kinetic experiments were performed using a procedure similar to the equilibrium studies. Samples containing adsorption studies were conducted in 250 mL shaking flasks at a solution pH of 7. The adsorbent dose of 0.2 g was thoroughly mixed with 50 mL of nickel solution (100 mg/L) and the suspensions were shaken at room temperature at required time intervals, filtered for the clear solutions, and analyzed for residual nickel ion concentration in the solutions. In order to determine the best kinetic model which fits the adsorption experimental data, the pseudo-first-order, pseudo-second-order, Elovich, and intraparticle diffusion models were examined.

3. Results and Discussion

3.1. Optimization of ZLRC Preparation

3.1.1. Effect of Independent Variables on ZLRC Preparation. According to the L$_{16}$ array designed by Taguchi method, 16

different ZLRC samples were prepared. The iodine number and yield of each sample were determined and shown in Table 2. The effect of operational parameters on responses of the prepared ZLRC samples is shown in Figure 1.

Effect of microwave radiation power (parameter A) on adsorption capacity and the yield of ZLRC were evaluated under the concentration of $ZnCl_2$ (X_{Zn}) of 30 mL and microwave radiation time of 4 min. Figure 1 shows that the yield of ZLRC samples was increased with the increasing of microwave power level from 100 to 400 W, and then decreased with the increasing of the level of 600 W. There were similar tendency of the iodine number on ZLRC. The possible reason was that the higher energy was offered to the samples with increasing the power level, the more active sites and pores on the samples. When microwave power reached a certain level, overfull energy could make a small quantity of carbon burnt, and the structure of pores was destroyed. Similar results have been obtained by other researchers [9, 20].

Effects of microwave radiation time (parameter B) on the yield and iodine number of ZLRC were evaluated, under the conditions of X_{Zn} of 30 mL and microwave power of 100 W (Figure 1). It revealed that the yield of ZLRC was increased with increasing the radiation time up to 8 min, and then decreased when the time was increased to 10 min. There were same tendency of the iodine number of ZLRC. Similar trends were also found by Li et al., when they prepared the activated carbon from tobacco stems using microwave radiation [21]. The activation degree was much more dependent on the microwave radiation time. With the prolongation of microwave radiation time, much more active sites and pores were formed on the surface of samples. Therefore the adsorption capacity of ZLRC would be increased with the prolongation of microwave radiation time. However, when microwave radiation time reached a certain value, the pores of carbon would be burnt off by microwave heating, which would lower the iodine number, the amount of nickel uptake, and the yield of ZLRC.

Under the microwave power of 100 W, radiation time of 8 min, the effects of the impregnation ratio (parameter C) of $ZnCl_2$ on the yield and iodine number of ZLRC were studied (Figure 1). With the increasing X_{Zn} from 30 mL to 90 mL, the yield, the iodine number, and the amount of MG adsorption of ZLRC were all increased. While X_{Zn} was further increased to 120 mL, these two parameters were all decreased. With increase in impregnation ratio, the initial effect of $ZnCl_2$ is to inhibit the release of volatile matter, which results in higher yield and iodine number of ZLRC. Subsequently, with the further increase in impregnation ratio, the zinc chloride assumed a dehydration agent role during activation. It inhibits the formation of tars and any other liquids that could clog up the pores of the sample; the movement of the volatiles through the pore passages would not be hindered; the volatiles will be subsequently released from the carbon surface during activation. Therefore the yield and iodine number of carbon were all decreased. Similar trends were also reported by Lua and Yang [22], Guo and Lua [23] in their studies on the preparation of activated carbon from pistachio-nut shell and oil-palm shells, respectively.
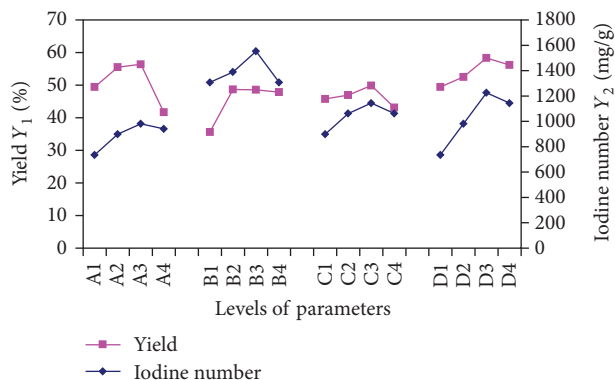

FIGURE 1: The effect of operational parameters on responses of the prepared ZLRC samples ((A) radiation power, (B) radiation time, (C) concentration of $ZnCl_2$, and (D) impregnation time).

The results presented in Figure 1 also shows that impregnation time (parameter D) had little influence on the yield and iodine number. The action of $ZnCl_2$ on the lignocellulosic material could be expressed as the following mechanism.

During impregnation stage the base attacked the cellular structure of *Ricinus communis* leaves, forming cleavage to the linkages between the lignin and cellulose. It was followed by recombination reactions, where larger structural units and strong cross linked solids were formed. This base worked, principally, in early stage during impregnation and might extended to have a slight effect in the carbonization stage [24].

3.1.2. Optimized Conditions. In the production of AC, relatively high product yield and adsorption capacity were expected. Therefore, more attention should be paid to improve the carbon yield and enhance its adsorption capacity for economical viability. However, it was difficult to optimize both these responses under the same condition, for the different interest in different region. From the discussions mentioned above, the microwave radiation power, microwave radiation time, impregnation ratio, and the impregnation time of $ZnCl_2$ had significant effects on the yield and the adsorption capacity of the activated carbon from *Ricinus communis* leaves with $ZnCl_2$ activation by microwave radiation. Therefore the optimum conditions were obtained as following: the microwave power of 100 W, microwave radiation time of 8 min, X_{Zn} of 30 mL, and impregnation time of 24 h. The iodine number and the yield of activated carbon prepared under optimum conditions were 58.18% and 1797.93 (mg/g), respectively. The ZLRC was used in the characterization analysis and adsorption experiments which were prepared under optimum conditions.

3.2. Characterization of ZLRC

3.2.1. Zero Surface Charges: The Characteristic Analysis of ZLRC. The zero surface charge characteristic of ZLRC was determined by using the solid addition method [19]. The experiment was conducted in a series of 250 mL glass stoppered flasks. Each flask was filled with 50 mL of different

initial pH NaNO$_3$ solutions and 0.2 g of ZLRC. The pH values of the NaNO$_3$ solutions were adjusted between 2 to 10 by adding either 0.1 M HNO$_3$ or 0.1 M NaOH. The suspensions were then sealed and shaken for 2 h at 150 rpm. The final pH values of the supernatant liquid were noted. The difference between the initial pH (pH$_i$) and final pH (pH$_f$) values (pH = pH$_i$ − pH$_f$) was plotted against the values of pH$_i$. The point of intersection of the resulting curve with abscissa, at which pH is 0, gave the pH$_{ZPC}$.

The pH$_{ZPC}$ of an adsorbent is a very important characteristic that determines the pH at which the adsorbent surface has net electrical neutrality. Figure 2 shows the plot between ΔpH, that is, (pH$_i$ − pH$_f$) and pH$_i$ for pH$_{ZPC}$ measurement. The point of zero charge for ZLRC is found to be 6.04. This result indicated that the pH$_{ZPC}$ of ZLRC depended on the raw material and the activated agency. The zero point charge (pH$_{ZPC}$ = 6.04 for ZLRC) is below the solution pH (pH = 7) and hence the negative charge density on the surface of ZLRC increased, which favours the adsorption of Ni^{2+} ions [25].

3.2.2. Functional Group Analysis of ZLRC. The aim of using FTIR analysis is to determine the existence of functional groups, and identification of characteristic peaks is based on the studies reported in the literature. The FTIR spectrum of ZLRC was shown in Figure 3.

The FTIR spectrum of ZLRC showed that the most predominant peaks in the spectrum originate from OH vibrations, CH$_2$, and CH$_3$ asymmetric and symmetric stretching vibrations. The intense bent at about 2927.94 cm^{-1} for the precursor was attributed to the asymmetric and symmetric vibration modes of methyl and methylene group [26]. The peak around 1651 cm^{-1} can be assigned to symmetric and asymmetric stretching vibrations of the C=C group. The band observed at 1396 cm^{-1} is associated to oxygen functionalities such as highly conjugated C–O stretching. The peaks at (1155–1033 cm^{-1}) region related to lignin. Therefore it is possible that cellulose, hemicelluloses, and lignin, having many OH groups in their structure, make up most of the absorbing layer. The peak present at 821 cm^{-1} indicates the presence of aromatic heterocyclic molecules.

3.2.3. XRD Analysis of ZLRC. Adsorption reaction may lead to changes in molecular and crystalline structure of the adsorbent and hence an understanding of the molecular and crystalline structures of the adsorbent and the resulting changes thereof would provide valuable information regarding adsorption reaction. Hence, XRD patterns of ZLRC before adsorption of Ni^{2+} ions have been studied.

As a representative case the XRD patterns of ZLRC before adsorption of Ni^{2+} ions are shown in Figure 4. The results indicated that the diffraction profiles of ZLRC exhibited broad peaks and the absence of a sharp peak revealed a predominantly amorphous structure; the broad peak seems to be appear at around $2\theta = 26°$ which was similar to the peak of crystalline carbonaceous structure such as graphite. From the XRD analysis for the adsorbent (ZLRC), we concluded that the activation was completed for the preparation of ZLRC as activated carbon.
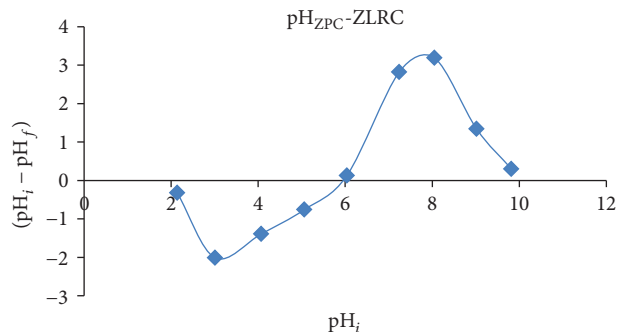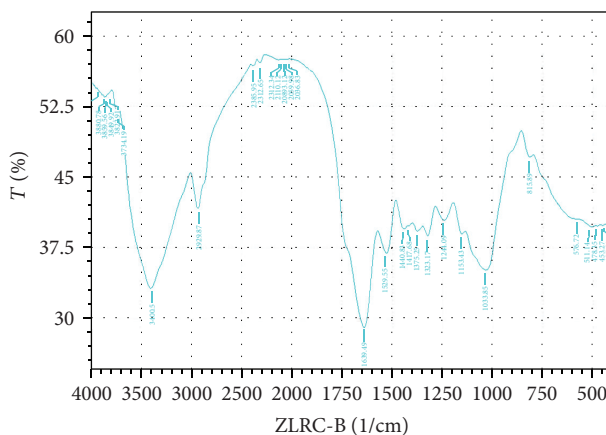

FIGURE 2: Zero point charges of ZLRC.

FIGURE 3: FTIR spectra of ZLRC.

3.3. Adsorption of Nickel Ion

3.3.1. The Effect of pH. The experiments carried out at different pH shows that there was a change in the percent removal of nickel ion over the entire pH range of 2 to 10 shown in Figure 5; pH is one of the most important parameters controlling the adsorption process. The effect of pH of the solution on the adsorption, desorption, and recycling ability of nickel ion on ZLRC was determined. The result is shown in Figure 5. The pH of the solution was controlled by the addition of 0.1 M HCl or 0.1 M NaOH. The uptake of nickel ion in aqueous solution was greatly affected by the variation of pH value, as shown in Figure 5. When the pH was lower than 3, the uptake went up sharply with the increase of pH. The maximum nickel ion uptake was obtained at 7 pH. At the initial metal ion concentration of 100 mg/L, removal efficiency was 9.03% at a solution pH of 2.0 for ZLRC, but it increased when solution pH increases from 2 to 7. At pH 7, the removal efficiency was 70.81% for ZLRC (pH$_{ZPC}$ = 6.04 for ZLRC). However, when the pH of the solution was increased from 7 to 10 the uptake of nickel ions was decreased. It appears that a change in pH of the solution results in the formation of different ionic species, and different carbon surface charge. At pH values lower than 5, the nickel ions can enter into the pore structure; this may be due to its small size.
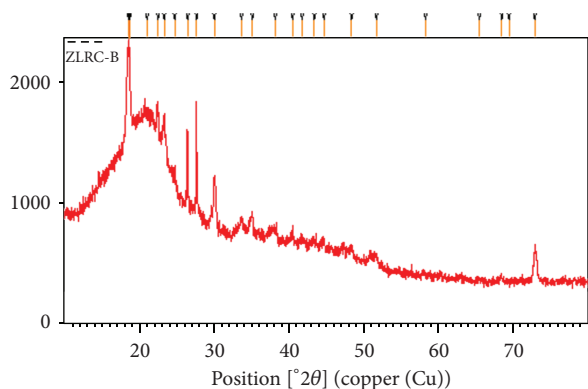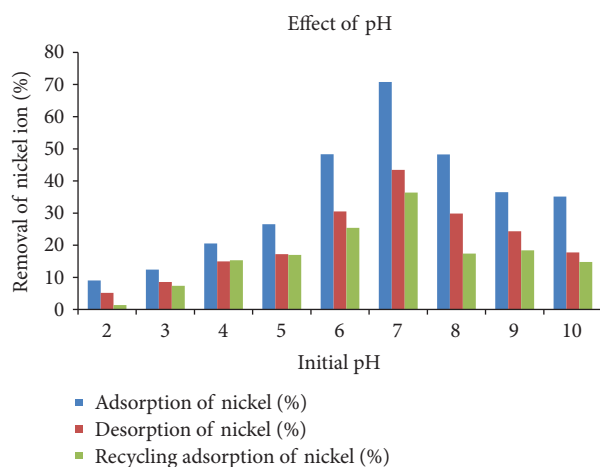
FIGURE 4: XRD analysis for ZLRC.

FIGURE 6: Effect of contact time on the adsorption of Ni^{2+} ions (100 mg/L of nickel, pH 7, and 0.2 g/50 mL of ZLRC).

FIGURE 5: Effect of pH on the adsorption, desorption, and recycling adsorption of Ni^{2+} ion. [Ni] = 1000 mg/L; contact time = 2 h; adsorbent dose = 0.2 g/50 mL.

FIGURE 7: Effect of adsorbent dose on the removal of Ni^{2+} ions onto ZLRC (Ni^{2+} concentration 100 mg/L, contact time 2 h, solution pH 7).

Desorption studies help to elucidate the nature of adsorption and recycling of the spent adsorbent and the nickel ion. If the adsorbed nickel ion can be desorbed using neutral pH water, then the attachment of the nickel ion of the adsorbent is by weak bonds. To study the effect of solution pH on nickel ion desorption, 50 mL of distilled water at different pH values (2–10) was agitated with 0.2 g of ZLRC in a mechanical orbital shaker at room temperature. The effect of pH on nickel ion desorption were studied by varying the pH from 2.0 to 9.0. The pH was adjusted with 0.1 M NaOH and 0.1 M HCl solutions. We could get maximum removal of 43.44% of adsorbed nickel ion for 7 pH water onto ZLRC, after 2 h of contact time between the loaded matrix and the desorbing agents.

Recycling ability of ZLRC was found to be maximum at pH 7. From the result it is evident that optimum pH of 7 is required for appreciable removal of nickel ions and hence this pH is employed as an optimum pH for further studies.

3.3.2. The Effect of Contact Time. The effect of time on the sorption of Ni^{2+} ions by *Ricinus communis* leaves was studied. Figure 6 indicates that the removal efficiency increased with
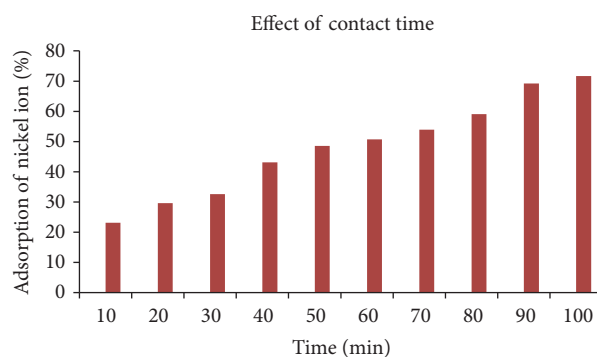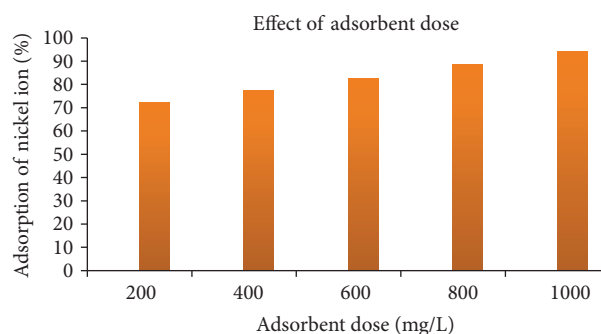
an increase in contact time before equilibrium is reached. This may be due to the attainment of equilibrium condition at 100 min of contact time for ZLRC, which is fixed as the optimum contact time. At the initial stage, the rate of removal of Ni^{2+} ions was higher, due to the availability of more than required number of active sites on the surface of carbons, and became slower at the later stages of contact time, due to the decreased or lesser number of active sites.

3.3.3. The Effect of Adsorbent Dosage. The influence of adsorbent dose on nickel ion removed at a fixed initial nickel concentration of 2 mg/L and pH 7 is shown in Figure 7. It was noticed that percentage removal of Ni^{2+} ion increased with an increase in adsorbent dose from 0.2 to 1 g/L. This was attributed to increased carbon surface and availability of more adsorption sites. From the result it is evident that optimum dosage of 0.2 g/50 mL is required for appreciable removal of Ni^{2+} ions and hence this amount is employed as a dose for further studies.

3.3.4. The Effect of Initial Nickel Ion Concentration. The experimental results of adsorption of Ni^{2+} ions on the activated carbon at various concentrations (10, 20, 30, and 40 mg/L) are shown in Figure 8. It reveals that the percentage of adsorption decreased with the increase in initial nickel
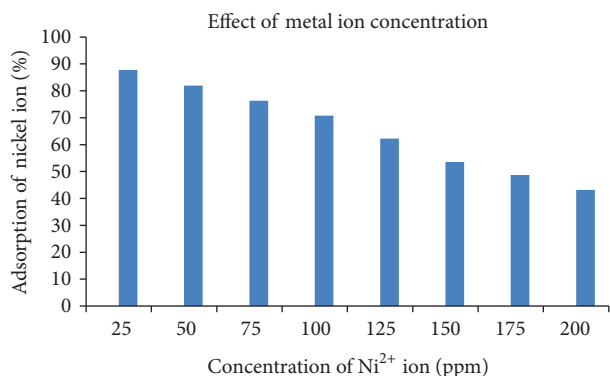
FIGURE 8: Effect of Initial concentration of Ni^{2+} ions on ZLRC. (Adsorbent dose 0.2 g/50 mL, contact time 2 h, solution pH 7).

- Ni = 100 mg/L, Cu = 10, 20, 30, and 40 mg/L
- Ni = 100 mg/L, Cr = 10, 20, 30, and 40 mg/L
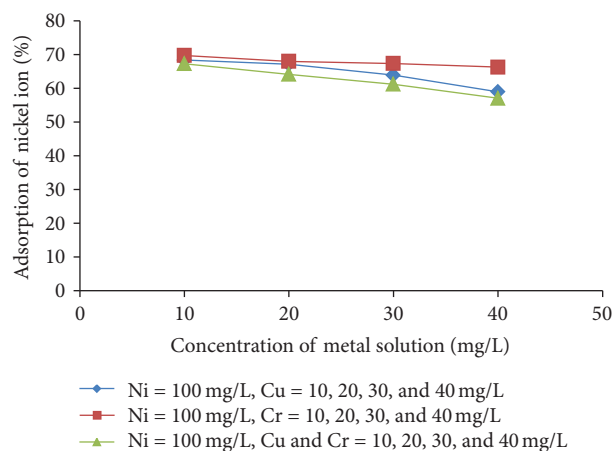- Ni = 100 mg/L, Cu and Cr = 10, 20, 30, and 40 mg/L

FIGURE 9: Effect of other ions on the adsorption of Ni^{2+} ions. (Adsorbent dose 0.2 g/50 mL, contact time 2 h, solution pH 7).

ion concentration. It means that the adsorption is highly dependent on initial concentration of nickel ion. That is why at lower concentration, the ratio of the initial number of nickel ion to the variable surface area is low, and subsequently the fractional adsorption becomes independent of initial concentration.

3.3.5. The Influence of Other Ions from Binary and Ternary Metal Solutions. Effects of the presence of Cu^{2+} and Cr^{3+} ions on the adsorption of Ni^{2+} ions were investigated by varying the concentrations of Cu^{2+} and Cr^{3+} ions from 10 mg/L to 40 mg/L. A comparison of the adsorption percentage of Ni^{2+} ions at equilibrium between the solutions with Ni^{2+} ions present as the single and with the presence of increasing concentration of Cu^{2+} and Cr^{3+} ions was given in Figure 9.

As shown in Figure 9, the results indicated that the equilibrium uptake of Ni^{2+} ions decreased with increasing concentration of Cu^{2+} and Cr^{3+} ions from 10 to 40 mg/L. In the single ion situation, the maximum uptake obtained at initial concentration of Ni^{2+} ions 100 mg/L, pH 7 was found to be 70.81%, while the uptake obtained in the binary (Ni-Cu and Ni-Cr) metal solutions at the same initial concentration of Ni^{2+} ions was found to be 70.41%, 67.18%, 63.91%, and 58.98% when the initial concentration of Cu^{2+} ion was 10, 20, 30, and 40 mg/L, respectively. Cr^{3+} ion in the binary solution slightly affect Ni^{2+} ion uptake on the ZLRC as much as Cu^{2+} ions (Figure 9). The maximum Ni^{2+} uptake obtained at the same conditions was found to be 69.76%, 68.02%, 67.39% and 66.29% when the concentration of Cr^{3+} ions was 10, 20, 30, and 40 mg/L, respectively.

As shown in Figure 9, the adsorption capacity of ZLRC for the ternary system with initial concentrations Ni^{2+}: 100 mg/L, Cu^{2+}: 10–40 mg/L, and Cr^{3+}: 10–40 mg/L, remained lower than that for the single metal ions and could be ascribed to the overlapping of biosorption sites of respective metal ions. The effect on the adsorption of other ions in ternary system of Ni^{2+} ion was found to be 67.32%, 64.16%, 61.23%, and 57.07% when the concentration of Cu^{2+} and Cr^{3+} ions was 10, 20, 30, and 40 mg/L.

A fixed quantity of nickel ion onto ZLRC could only offer a finite number of surface binding sites, some of which would be expected to be saturated by the competing metal solutions. The decrease in sorption capacity of the same activated carbon in target metal solution than that of single metal may be ascribed to the less availability of binding sites. In case of binary and ternary metal solution, the binding site is competitively divided among the various metal ions.

It is generally complicated to find a common rule to identify how metal properties affect the competitive sorption. Among various factors that affect the sorption preferences of a sorbent, binding of metal ions on material largely depends on physicochemical properties of metals.

The HSAB (hard and soft acids and bases) theory was developed by Pearson [27] and extended to activated carbons adsorption by Alfarra et al. [28]. Once acids and bases have been classified as hard or soft, a simple rule of the HSAB principle can be given; hard acids prefer to bond to hard bases, and soft acids prefer to bond to soft bases. Generally, the C–O or C=O bonds are more polar and less polarizable, hence harder than the C–C or C=C bonds. In this concept, the oxygen surface groups of ZLRC are the hard sites that fix hard metal ions. According to this theory, Ni^{2+}, Cu^{2+}, and Cr^{3+} cations are borderline acids [27]. Changing the experimental conditions, metal ions with a borderline hardness can be biosorbed by the hard sites of ZLRC. The cationic exchange between the oxygenated surface groups (hard base) of ZLRC and borderline acids gives ionic bonds which are more easily dissociated. But the competitive process cannot be explained exactly by the hardness of cations because other effective factors and hardness values of Ni^{2+}, Cu^{2+}, and Cr^{3+} borderline acids are close to each other.

It has been reported that in general, the greater the atomic weight, electronegativity, electrode potential, and ionic size, the greater will be the affinity for sorption [29]. Electronegativities and ionic radius of the elements are given in Table 3. It is clear that electronegativity is dominant factor for biosorption.

3.4. Adsorption Isotherms. Langmuir, Freundlich, Temkin, and Dubinin-Radushkevich isotherm models are frequently used for estimating the quantification of the adsorptive capacity of ZLRC.

Langmuir [30] proposed a theory to describe the adsorption of gas molecules onto metal surfaces. The Langmuir adsorption isotherm has been successfully applied to many real sorption processes. Langmuir isotherm [31] assumes monolayer adsorption onto a surface containing a finite number of adsorption sites. It also assumes uniform energies of adsorption onto the surface without transmigration of adsorbate in the plane of the surface [32]. Therefore, the Langmuir isotherm model was chosen for estimation of the maximum adsorption capacity corresponding to complete monolayer coverage on the adsorbent surface. The Langmuir nonlinear equation is commonly expressed as follows:

$$q_e = \frac{Q_m K_L C_e}{1 + K_L C_e}. \tag{3}$$

In (3) C_e and q_e are defined as before in (2), Q_m is a constant and reflects a complete monolayer (mg/g), and K_L is adsorption equilibrium constant (L/mg) that is related to the apparent energy of sorption. The Langmuir isotherm (3) can be linearized into the following form [33, 34]:

$$\frac{C_e}{q_e} = \frac{1}{K_L Q_m} + \frac{1}{Q_m} \times C_e. \tag{4}$$

A plot of C_e/q_e versus C_e should indicate a straight line of slope $1/Q_m$ and an intercept of $1/K_L Q_m$. The results obtained from the Langmuir for the removal of Ni^{2+} ions onto ZLRC are shown in Table 4. The correlation coefficients reported in Table 4 showed strong positive evidence on the adsorption of Ni^{2+} ions onto ZLRC following the Langmuir isotherm. The applicability of the linear form of Langmuir model to ZLRC was proved by the high correlation coefficients $R^2 = 0.999$. This suggests that the Langmuir isotherm provides a good model of the sorption system. The maximum monolayer capacity Q_m obtained from the Langmuir is 250 mg/g.

The Freundlich isotherm is an empirical equation assuming that the adsorption process takes place on a heterogeneous surface through a multilayer adsorption mechanism and adsorption capacity is related to the concentration of metal at equilibrium [35]. The Freundlich equation is given as

$$q_e = K_f C_e^{1/n}, \tag{5}$$

where q_e is the amount of adsorbate adsorbed at equilibrium (mg/g), C_e is the equilibrium concentration of the adsorbate (mg/L), K_f is the Freundlich adsorption constant related to adsorption capacity of the adsorbent ($(mg/g) (L/mg)^{1/n}$), and $1/n$ is the adsorption intensity. A linear form of the Freundlich equation is generally expressed (5) as follows:

$$\ln q_e = \ln K_f + \frac{1}{n} \ln C_e. \tag{6}$$

The values of K_f and $1/n$ were calculated from the intercept and slope of the plot of $\log q_e$ versus $\log C_e$. The applicability

TABLE 3: Electronegativities and ionic radius of Ni^{2+}, Cu^{2+}, and Cr^{3+} ions.

Ion	Ionic radius (pm)	Electronegativity (Pauling scale)
Ni^{2+}	83	1.75
Cu^{2+}	73	1.90
Cr^{3+}	75.5	1.66

of the Freundlich adsorption isotherm was also analyzed, using the same set of experimental data, by plotting $\log q_e$ versus $\log C_e$. The data obtained from linear Freundlich isotherm plot for the adsorption of nickel onto ZLRC was showed in Table 4. The correlation coefficient (0.9280) showed that the Freundlich model is comparable to the Langmuir model. The $1/n$ is lower than 1.0, indicating that Ni^{2+} ion is favorably adsorbed by ZLRC.

Temkin and Pyzhev considered the effects of some indirect sorbate/adsorbate interactions on adsorption isotherms and suggested that because of these interactions the heat of adsorption of all molecules in the layer would decrease linearly with coverage [36]. The Temkin isotherm has been used in the following form:

$$q_e = \frac{RT}{b} \ln \left(K_T C_e \right), \tag{7}$$

where K_T is the equilibrium binding constant (L/g), b is related to heat of adsorption (J/mol), R is the universal gas constant (8.314 J/mol K), and T is the absolute temperature (K).

Equation (7) can be written as the following form

$$q_e = B_1 \ln \left(K_T C_e \right). \tag{8}$$

The Temkin adsorption isotherm parameters are calculated and the values are summarized in Table 4. The adsorption data were analyzed according to the linear of the Temkin isotherm. Examination of the data shows that the Temkin isotherm fitted well the Ni^{2+} ion adsorption data for ZLRC. The heat of Ni^{2+} ion adsorption onto ZLRC was found to be 54.811 KJ/mol. The correlation coefficient R^2 obtained from Temkin model was comparable to that obtained for Langmuir and Freundlich equations, which explains the applicability of Temkin model to the adsorption of Ni^{2+} ions onto ZLRC.

The Dubinin-Radushkevich (D-R) equation can be expressed [37] as

$$q_e = q_m e^{-K' \varepsilon^2}, \tag{9}$$

where ε (Polanyi potential) is equal to $RT \ln(1 + 1/C_e)$, q_e is the amount of nickel adsorbed per unit activated carbon (mol/g), q_m is the theoretical monolayer saturation capacity (mol/g), C_e is the equilibrium concentration of the metal solution (mol/L), K' is the constant of the adsorption energy (mol^2/kJ^2), R the gas constant (kJ/mol K), and T is the temperature (K). The linear form of the D-R isotherm is

$$\ln q_e = \ln q_m - K' \varepsilon^2. \tag{10}$$

TABLE 4: Adsorption isotherm parameters for adsorption of Ni^{2+} ions onto ZLRC.

Isotherm model	Parameters	
Langmuir	Q_m (mg g^{-1})	250
	b (L mg^{-1})	0.0851
	R^2	0.9990
Freundlich	$1/n$	0.3777
	K_f (mg g^{-1})	41.1147
	R^2	0.9280
Temkin	α (L g^{-1})	0.0611
	β (mg L^{-1})	45.960
	b	54.811
	R^2	0.9790
Dubinin-Radushkevich	Q_m (mg g^{-1})	177.237
	K ($\times 10^{-5}$ mol^2 kJ^{-2})	1.0000
	E (kJ mol^{-1})	0.0709
	R^2	0.8310

K' is related to mean adsorption energy (E, kJ/mol) as [38]

$$E = \frac{1}{\sqrt{2K'}}. \qquad (11)$$

The constant obtained from D-R isotherms are shown in Table 4. The mean adsorption energy (E) gives information about chemical and physical adsorption [39]. The value of E was found to be 0.0709 KJ/mol, which indicates that the physicosorption process plays the significant role in the adsorption of Ni^{2+} ions onto ZLRC.

The equilibrium isotherms was studied by varying the initial concentration of Ni^{2+} ions under the conditions of pH 7.0, contact time 2 h, and activated carbon dose 0.2 g/mL. Adsorption isotherm models adopted in this work and their parameters are presented in Table 4. The fitting results, that is, isotherm parameters and the coefficient of determination, R^2 values, were shown in Table 4. According to a linear regression method, the Freundlich, Temkin and Dubinin-Radushkevich isotherms were poorly suitable to the adsorption of ZLRC in comparison to Langmuir isotherm. The validity of the Langmuir model suggested that the metal uptake was due to monolayer coverage of solute particles onto the surface of the activated carbon and adsorption of each molecule has equal activation energy.

3.5. Adsorption Kinetics.

Pseudo-first-order, pseudo-second-order, Elovich, and intraparticle diffusion models were used to test the experimental data and thus explain the adsorption kinetic process. The procedure of adsorption kinetic was identified to adsorption equilibrium, were withdrawn at time intervals and the concentrations of Ni^{2+} ions were similarly measured.

The pseudo-first-order equation of Lagergren is generally expressed as follows [40, 41]:

$$\frac{dq_t}{dt} = k_1 (q_e - q_t). \qquad (12)$$

After integration and applying boundary conditions, $t = 0$ to $t = t$ and $q_t = 0$ to $q_t = q_t$ the integrated form of the above equation becomes

$$q_t = q_e \left(1 - e^{-K_1 t}\right). \qquad (13)$$

However, (13) is transformed into its linear form for use in the kinetic analyses of data

$$\ln (q_e - q_t) = \ln q_e - k_1 t, \qquad (14)$$

where q_e (mg/g) and q_t (mg/g) are the amount of adsorbed adsorbate at equilibrium and at time t, respectively, and k_1 (1/min) is the rate constant of pseudo first-order adsorption. The straight line plots of log $(q_e - q_t)$ against t of (14) were made at room temperature. The parameters were summarized in Table 5. From the linear correlation coefficients (R^2), it is seen that Lagergren equation does not represent a good fit with the experimental data.

If the rate of adsorption has a second-order mechanism, the pseudo-second-order chemisorption kinetic rate equation is expressed as

$$\frac{t}{q_t} = \frac{1}{k q_e^2} + \frac{1}{q_e} t, \qquad (15)$$

where q_e and q_t are the sorption capacities at equilibrium and at time t, respectively, (mg/g) and k is the rate constant of pseudo-second-order sorption (g/mg/min). Where h can be regarded as the initial sorption rate as q_t/t tents to zero, hence:

$$h = k q_e^2. \qquad (16)$$

Equation (16) can be written as

$$\frac{t}{q_t} = \frac{1}{h} + \frac{1}{q_e} \times t. \qquad (17)$$

Equation (17) does not have the disadvantage of the problem with assigning an effective q_e. If pseudo-second-order

TABLE 5: Comparison of the correlation coefficients of kinetic parameters for the adsorption of Ni^{2+} ions onto ZLRC.

Models	Parameters	
Pseudo-first-order model	k_1 (min^{-1})	0.0253
	q_e (mg/g)	181.130
	R^2	0.821
Pseudo-second-order model	k_2 (g/mg/min)	0.0207
	q_e (mg/g)	250.0
	h	5.1800
	R^2	0.9020
Intra-particle diffusion model	k_{dif} (mg/(g·min$^{1/2}$))	17.11
	C	5.2520
	R^2	0.960
Elovich model	A_E (mg (g/min))	0.0217
	b (g/mg)	4.0768
	R^2	0.8750

kinetics is applicable, the plot of t/q_t against t of (16) should give a linear relationship. Values of q_e, k and h can be determined from the slope and intercept of the plots of $1/q_t$ versus t. The linear plots of t/q_t versus t show good agreement between experimental and calculated q_e values. The linear correlation coefficient for the second-order kinetic model was obtained to be 0.9020, which led to believe that the Pseudo-second order kinetic model provided good correlation for the adsorption of Ni^{2+} ions onto ZLRC.

The adsorption of Ni^{2+} ions onto ZLRC may be controlled by via external flim diffusion at earlier stages and later by the particle diffusion. The possibility of intraparticle diffusion resistance was identified by using the following intraparticle diffusion model as [42]

$$q_t = K_{\text{dif}} t^{1/2} + C, \qquad (18)$$

where K_{dif} is the intraparticle diffusion rate constant (mg/ (g·min$^{1/2}$)), C is the intercept. The values of q_t were found to be correlated linearly with values of $t^{1/2}$ and the rate constant K_{dif} directly evaluated from the slope of regression line (Table 5). The values of C provide information about the thickness of the boundary layer. The constant C was found to be 5.2520. The R^2 values given in Table 5 are close to unity indicating the application of this model. This may confirm that the rate-limiting step is the intraparticle diffusion process. The linearity of the plots demonstrated that intraparticle diffusion played a significant role in the uptake of the adsorbate by adsorbent. As still there is no significant indication about it, Ho [43] has shown that if the intraparticle diffusion is the sole rate-limiting step, it is essential for the q_t versus $t^{1/2}$ plots to pass through the origin, which is not the case; it may be concluded that surface adsorption and intraparticle diffusion were concurrently operating during the Ni^{2+} ions and ZLRC interactions.

The Elovich equation is another rate equation based on the adsorption capacity generally expressed as follows:

$$\frac{dq_t}{dt} = B_E \exp^{-(A_E q_t)}, \qquad (19)$$

where B_E is the initial adsorption rate constant (mg (g/min)) and A_E is the desorption constant (g/mg) during any experiment.

It is simplified by assuming $A_E B_E t \gg t$ and by applying the boundary conditions $q_t = 0$ at $t = 0$ and $qt = t$ at $t = t$, (19) becomes

$$q_t = \frac{1}{A_E}\left(B_E A_E\right) + \frac{1}{A_E}\ln t. \qquad (20)$$

If Ni^{2+} ion adsorption by ZLRC fits the Elovich model, a plot of q_t versus $\ln(t)$ should yield a linear relationship with a slope of $(1/A_E)$ and an intercept of $(1/A_E)\ln(A_E B_E)$. Thus, the constants can be obtained from the slope and the intercept of the straight line. The calculated parameters were presented in Table 5.
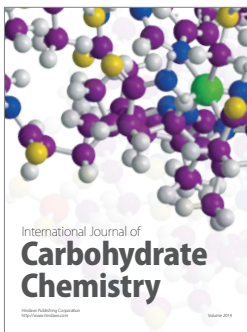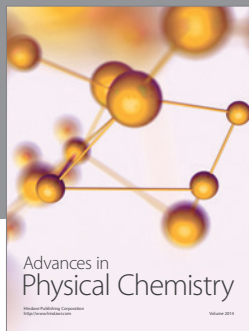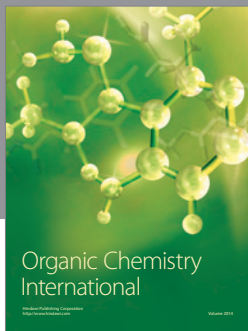
4. Conclusion

It had indicated that $ZnCl_2$ was a suitable activating agent for the preparation of ZLRC by microwave radiation. Taguchi method was used to optimize the preparation conditions of ZLRC. Radiation time and concentration of $ZnCl_2$ were significant factors for ZLRC yield. Concentration of $ZnCl_2$ was the greatest impact factor on iodine number of ZLRC. The optimum conditions were radiation power of 100 W, radiation time of 8 min, concentration of $ZnCl_2$ of 30% by volume, and the impregnation time of 24 h. The yield and iodine number of ZLRC were 58.18% and 1797.93 mg/g. Langmuir isotherm better fits the experimental equilibrium data of nickel adsorption on the prepared ZLRC. The influence of binary and ternary mixture of heavy metal solution onto the surface of ZLRC was found to be competitive where the percentage adsorption of metals with those of single metal ions. The maximum nickel adsorption capacity on ZLRC is 250 mg/g. The data indicate that the adsorption kinetics follows the pseudo-second-order rate with intraparticle diffusion as one of the rate determining steps. The present

study concludes that the ZLRC could be employed as low-cost adsorbent as alternative to commercial activated carbon for the removal of metals from water and waste water.

References

[1] F. Rozada, M. Otero, A. Morán, and A. I. García, "Adsorption of heavy metals onto sewage sludge-derived materials," *Bioresource Technology*, vol. 99, no. 14, pp. 6332–6338, 2008.

[2] K. K. Krishnani, X. Meng, C. Christodoulatos, and V. M. Boddu, "Biosorption mechanism of nine different heavy metals onto biomatrix from rice husk," *Journal of Hazardous Materials*, vol. 153, no. 3, pp. 1222–1234, 2008.

[3] D. Feng, C. Aldrich, and H. Tan, "Treatment of acid mine water by use of heavy metal precipitation and ion exchange," *Minerals Engineering*, vol. 13, no. 6, pp. 623–642, 2000.

[4] C. P. Huang and D. W. Blankenship, "The removal of mercury (II) from dilute aqueous solution by activated carbon," *Water Research*, vol. 18, no. 1, pp. 37–46, 1984.

[5] S. Babel and T. A. Kurniawan, "Low-cost adsorbents for heavy metals uptake from contaminated water: a review," *Journal of Hazardous Materials*, vol. 97, no. 1–3, pp. 219–243, 2003.

[6] J. Hayashi, A. Kazehaya, K. Muroyama, and A. P. Watkinson, "Preparation of activated carbon from lignin by chemical activation," *Carbon*, vol. 38, no. 13, pp. 1873–1878, 2000.

[7] A. T. Mohd Din, B. H. Hameed, and A. L. Ahmad, "Batch adsorption of phenol onto physiochemical-activated coconut shell," *Journal of Hazardous Materials*, vol. 161, no. 2-3, pp. 1522–1529, 2009.

[8] C. Almansa, M. Molina-Sabio, and F. Rodríguez-Reinoso, "Adsorption of methane into $ZnCl_2$-activated carbon derived discs," *Microporous and Mesoporous Materials*, vol. 76, no. 1–3, pp. 185–191, 2004.

[9] W. Li, L. B. Zhang, J. H. Peng, N. Li, and X. Y. Zhu, "Preparation of high surface area activated carbons from tobacco stems with K_2CO_3 activation using microwave radiation," *Industrial Crops and Products*, vol. 27, no. 3, pp. 341–347, 2008.

[10] P. T. Williams and A. R. Reed, "Development of activated carbon pore structure via physical and chemical activation of biomass fibre waste," *Biomass and Bioenergy*, vol. 30, no. 2, pp. 144–152, 2006.

[11] M. Molina-Sabio and F. Rodríguez-Reinoso, "Role of chemical activation in the development of carbon porosity," *Colloids and Surfaces A*, vol. 241, no. 1–3, pp. 15–25, 2004.

[12] M. C. Basso, E. G. Cerrella, and A. L. Cukierman, "Activated carbons developed from a rapidly renewable biosource for removal of cadmium(II) and nickel(II) ions from dilute aqueous solutions," *Industrial and Engineering Chemistry Research*, vol. 41, no. 2, pp. 180–189, 2002.

[13] J. Guo and A. C. Lua, "Characterization of adsorbent prepared from oil-palm shell by CO_2 activation for removal of gaseous pollutants," *Materials Letters*, vol. 55, no. 5, pp. 334–339, 2002.

[14] T. Budinova, E. Ekinci, F. Yardim et al., "Characterization and application of activated carbon produced by H_3PO_4 and water vapor activation," *Fuel Processing Technology*, vol. 87, no. 10, pp. 899–905, 2006.

[15] C. O. Ania, J. B. Parra, J. A. Menéndez, and J. J. Pis, "Effect of microwave and conventional regeneration on the microporous and mesoporous network and on the adsorptive capacity of activated carbons," *Microporous and Mesoporous Materials*, vol. 85, no. 1-2, pp. 7–15, 2005.

[16] J. M. V. Nabais, P. J. M. Carrott, M. M. L. R. Carrott, and J. A. Menéndez, "Preparation and modification of activated carbon fibres by microwave heating," *Carbon*, vol. 42, no. 7, pp. 1315–1320, 2004.

[17] D. A. Jones, T. P. Lelyveld, S. D. Mavrofidis, S. W. Kingman, and N. J. Miles, "Microwave heating applications in environmental engineering—A review," *Resources, Conservation and Recycling*, vol. 34, no. 2, pp. 75–90, 2002.

[18] H. Deng, G. Zhang, X. Xu, G. Tao, and J. Dai, "Optimization of preparation of activated carbon from cotton stalk by microwave assisted phosphoric acid-chemical activation," *Journal of Hazardous Materials*, vol. 182, no. 1–3, pp. 217–224, 2010.

[19] A. Kumar, B. Prasad, and I. M. Mishra, "Adsorptive removal of acrylonitrile by commercial grade activated carbon: kinetics, equilibrium and thermodynamics," *Journal of Hazardous Materials*, vol. 152, no. 2, pp. 589–600, 2008.

[20] H. Deng, L. Yang, G. Tao, and J. Dai, "Preparation and characterization of activated carbon from cotton stalk by microwave assisted chemical activation-Application in methylene blue adsorption from aqueous solution," *Journal of Hazardous Materials*, vol. 166, no. 2-3, pp. 1514–1521, 2009.

[21] W. Li, L.-B. Zhang, J. H. Peng, N. Li, and X. Y. Zhu, "Preparation of high surface area activated carbons from tobacco stems with K_2CO_3 activation using microwave radiation," *Industrial Crops and Products*, vol. 27, no. 3, pp. 341–347, 2008.

[22] A. C. Lua and T. Yang, "Characteristics of activated carbon prepared from pistachio-nut shell by zinc chloride activation under nitrogen and vacuum conditions," *Journal of Colloid and Interface Science*, vol. 290, no. 2, pp. 505–513, 2005.

[23] J. Guo and A. C. Lua, "Textural characterization of activated carbons prepared from oil-palm stones pre-treated with various impregnating agents," *Journal of Porous Materials*, vol. 7, no. 4, pp. 491–497, 2000.

[24] A. N. A. El-Hendawy, A. J. Alexander, R. J. Andrews, and G. Forrest, "Effects of activation schemes on porous, surface and thermal properties of activated carbons prepared from cotton stalks," *Journal of Analytical and Applied Pyrolysis*, vol. 82, no. 2, pp. 272–278, 2008.

[25] P. Janoš, H. Buchtová, and M. Rýznarová, "Sorption of dyes from aqueous solutions onto fly ash," *Water Research*, vol. 37, no. 20, pp. 4938–4944, 2003.

[26] K. Nakanishi, *Infrared Absorption Spectroscopy-Practical*, Holden-Day, San Francisco, CA, 1962.

[27] R. G. Pearson, "Hard and soft acids and bases," *Journal of the American Chemical Society*, vol. 85, no. 22, pp. 3533–3539, 1963.

[28] A. Alfarra, E. Frackowiak, and F. Béguin, "The HSAB concept as a means to interpret the adsorption of metal ions onto activated carbons," *Applied Surface Science*, vol. 228, no. 1–4, pp. 84–92, 2004.

[29] Y. Sag, B. Akeael, and T. Kutsal, "Ternary biosorption equilibria of Cr(VI) Cu(II) and Cd(II) on *Rhizopus arrihzus*," *Separation Science and Technology*, vol. 37, pp. 279–309, 2002.

[30] I. Langmuir, "The adsorption of gases on plane surfaces of glass, mica and platinum," *The Journal of the American Chemical Society*, vol. 40, no. 9, pp. 1361–1403, 1918.

[31] I. Langmuir, "The constitution and fundamental properties of solids and liquids. Part I. Solids," *The Journal of the American Chemical Society*, vol. 38, no. 2, pp. 2221–2295, 1916.

[32] M. Doğan, M. Alkan, and Y. Onganer, "Adsorption of methylene blue from aqueous solution onto perlite," *Water, Air, and Soil Pollution*, vol. 120, no. 3-4, pp. 229–248, 2000.

[33] D. G. Kinniburgh, "General purpose adsorption isotherms," *Environmental Science and Technology*, vol. 20, no. 9, pp. 895–904, 1986.

[34] E. Longhinotti, F. Pozza, L. Furlan et al., "Adsorption of anionic dyes on the biopolymer chitin," *Journal of the Brazilian Chemical Society*, vol. 9, no. 5, pp. 435–440, 1998.

[35] H. M. F. Freundlich, "Over the adsorption in solution," *Journal of Physical Chemistry*, vol. 57, pp. 385–470, 1906.

[36] M. J. Temkin and V. Pyzhev, "Recent modifications to Langmuir isotherms," *Acta Physiochimica URSS*, vol. 1, pp. 217–222, 1940.

[37] B. Acemioğlu, "Adsorption of Congo red from aqueous solution onto calcium-rich fly ash," *Journal of Colloid and Interface Science*, vol. 274, no. 2, pp. 371–379, 2004.

[38] HOBSON JP, "Physical adsorption isotherms extending from ultrahigh vacuum to vapor pressure," *Journal of Physical Chemistry*, vol. 73, no. 8, pp. 2720–2727, 1969.

[39] W. Riemam and H. Walton, *Ion Exchange in Analytical Chemistry*, vol. 38 of *International Series of Monographs in Analytical Chemistry*, Pergamon Press, Oxford, UK, 1970.

[40] G. Crini, H. N. Peindy, F. Gimbert, and C. Robert, "Removal of C.I. Basic Green 4 (Malachite Green) from aqueous solutions by adsorption using cyclodextrin-based adsorbent: kinetic and equilibrium studies," *Separation and Purification Technology*, vol. 53, no. 1, pp. 97–110, 2007.

[41] M. Özacar and I. A. Şengil, "A kinetic study of metal complex dye sorption onto pine sawdust," *Process Biochemistry*, vol. 40, no. 2, pp. 565–572, 2005.

[42] W. J. Weber and J. C. Morris, "Kinetics of adsorption on carbon from aqueous solution," *Journal of the Sanitary Engineering Division*, vol. 89, pp. 31–59, 1963.

[43] Y. S. Ho, "Removal of copper ions from aqueous solution by tree fern," *Water Research*, vol. 37, no. 10, pp. 2323–2330, 2003.